JOURNAL OF APPLIED ELECTROCHEMISTRY 11 (1981) 335–338

Electrolyte limitations in molten salt batteries

M. J. WILLARS, J. G. SMITH, R. W. GLAZEBROOK

Shell Research Limited, Thornton Research Centre, PO Box 1, Chester, UK

Received 22 July 1980

A pelletized LiAl–FeS battery employing an immobilized LiCl–KCl electrolyte has been tested under various operating regimes. The ampere-hour capacity of cells was found to be inversely proportional to discharge rate. This behaviour has been interpreted in terms of electrolyte phase separation in regions near to the surface of the iron sulphide electrode. Further evidence was provided by the temperature dependence of active materials utilization. Close agreement was obtained between predicted results and experimental data.

1. Introduction

Attempts to develop high-energy-density batteries have led many researchers to investigate high-temperature systems based on alkali metal electrodes. In recent years much attention (particularly in the US) has been focused on the secondary lithium–sulphur couple described in the 1960s by the Argonne National Laboratory [1]. The containment and corrosion problems associated with using these elements in the molten state have been mitigated by manufacturing electrodes from lithium–aluminium alloys and iron sulphide. The discharge reaction

$$2\mathrm{Li(Al)} + \mathrm{FeS} \longrightarrow \mathrm{Li_2S} + \mathrm{Fe} + 2\mathrm{Al} \qquad (1)$$

occurs at a potential of $\simeq 1.30$ V and the system has a theoretical energy density of 456 W h kg^{-1}.

In early free-electrolyte cell designs, a molten lithium chloride–potassium chloride eutectic mixture filled the space between the electrodes which were separated by an inert woven cloth (typically of boron nitride). Such cells have been shown to have high energy densities and to deliver high power [2, 3], but the cost of separator materials and the complexity of construction represent considerable economic disadvantages.

A much simpler cell design which eliminates the need for expensive ceramic separators has been described by the UK Admiralty Marine Technology Establishment [4, 5]. The cell is manufactured in the form of a pressure-compacted pellet, the electrolyte being immobilized by admixture with an inert powder. Cells constructed in this way have been shown to have outstanding lifetimes of > 2000 cycles [6]. Magnesia (MgO), with its high stability and low cost, is considered to be one of the most promising filler materials for use in Li–S cells [7], and is currently under investigation in several laboratories [8, 9]. However, the relatively small amount of electrolyte contained within the porous matrix of the electrodes leads to the possibility of electrolyte limitations on cell performance. Braunstein and Vallet [10, 11] have shown from migration and diffusion equations that phase separation can occur in mixed cationic electrolytes. They have measured the separation of components in the system $AgNO_3$–KNO_3 when high currents have been passed between silver electrodes [12].

This paper describes experiments that provide quantitative electrochemical evidence for the existence of phase separation at the electrodes of LiAl–FeS cells during discharge.

2. Experimental

The fundamental concepts behind the immobilized-electrolyte, pelletized cell have been described elsewhere [4], and the cell constituents are listed in Table 1. A lithium chloride–potassium chloride eutectic mixture was used as the electrolytic medium. This was mixed with magnesium oxide powder to form the basic electrolyte material. The active electrode components were iron sulphide, ground to less than 75 μm, and a 20 wt% lithium–

0021–891X/81/030335–04$02.40/0

Table 1. Electrode and electrolyte constituents. Electrolyte ≡ 70% MgO plus 30% LiCl–KCl eutectic mixture

	Li–Al	*FeS*	*Electrolyte*	*Weight* (g)
Positive electrode	–	70%	30%	1.45
Electrolyte layer	–	–	100%	3.00
Negative electrode	70%	–	30%	1.40

aluminium alloy, used as supplied. All of the chemicals were dried in a vacuum furnace prior to use and subsequently handled in an argon-atmosphere glove-box.

Sandwich-type disc cells (8.3 cm^2 nominal surface area) were constructed by pressing the appropriate amounts of material in a die at 30 000 lbf in^{-2} (207 MN m^{-2}) and ambient temperature, generally in a single operation. The cells were housed in stainless steel bolt-up units, and were insulated from the walls by a fused MgO insulating ring. Molybdenum current collectors were used. Testing was performed using battery cycling units (which induced current reversal at pre-set potential limits) in conjunction with constant current sources, and data were recorded on *Y–t* recorders.

The cell capacities could be calculated from the time required to sweep between two voltage limits at a known charge–discharge rate, and the total energy passed was determined from a voltage integration trace on the *Y–t* recorder. All cells were cycled at least 50 times before the imposition of a new operating regime and tests were carried out over a further 50-cycle period. After the test period had been completed the units were returned to the initial conditions (450° C, 25 mA cm^{-2}† charge and discharge) in order to confirm that no irreversible cell changes had occurred.

3. Results and discussion

A typical cell charge–discharge profile between potential limits of 0.9 V and 1.7 V is shown in Fig. 1. The coulombic efficiency of such cells (i.e. the charge passed during discharge ÷ charge passed during the charging process) is essentially 100% and the overall energy efficiency greater than 80%. Changes in slope of the potential–time plot near

† Calculated from the nominal electrode surface area.

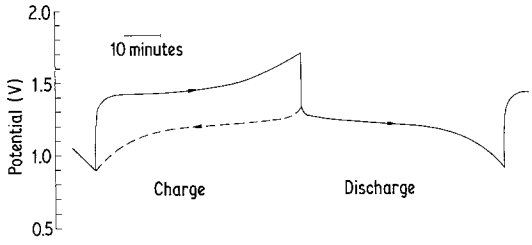

Fig. 1. Typical charge–discharge cycle for a LiAl–FeS cell at 450° C ($i_{charge} = i_{discharge} = 25$ mA cm^{-2}).

the end of charge and discharge are accompanied by an increase in the measured cell resistance (as determined by a current interruption technique). Such observations could be attributed to a 'freezing-out' of electrolyte near to the electrode surfaces where local concentration changes will occur.

Fig. 2 illustrates the effect of variation in discharge current on cell capacities (and hence on the utilization of active materials present). It is clear from these data that for a constant charge rate of 25 mA cm^{-2} at 450° C, the discharge current limits the cell capacity. At a discharge rate of 12.5 mA cm^{-2} a utilization figure of about 55% is obtained, whereas at a discharge rate of 50 mA cm^{-2} a 16% utilization is recorded. This behaviour

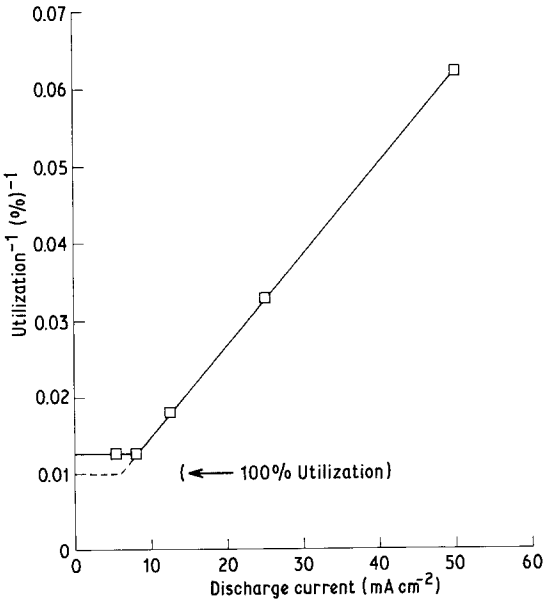

Fig. 2. Effect of discharge current density on utilization of active electrode materials ($T = 450°$ C, $i_{charge} = 25$ mA cm^{-2}).

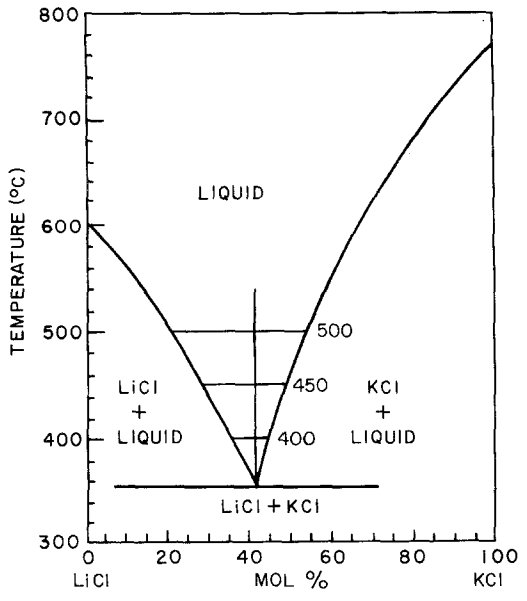

Fig. 3. Phase diagram for the lithium chloride–potassium chloride system.

is typical of battery systems in that whenever a high current is withdrawn (i.e. in a high-power application) the capacity is reduced. The capacity–power relationship for this system can be interpreted by reference to Fig. 3, the electrolyte phase diagram. Whenever a current is passed through the cell, lithium ions are released into the electrolyte at one electrode and removed at the other. Concentration gradients are built up near to the electrode surface, resulting in localized composition changes in the electrolyte. Once the composition has changed by a certain critical amount (indicated by the point where a constant temperature line crosses the phase boundary in Fig. 3) the electrolyte freezes, increasing the solution resistance of the cell and physically blocking reaction sites. It is clear from the liquid boundaries in the phase diagram that a smaller composition change (from the initial eutectic composition) is required to reach this critical point when the lithium content is decreasing rather than increasing. For electrodes of similar surface area this condition will be realized at the lithium–aluminium electrode during charge and at the ferrous sulphide electrode during discharge. The curve in Fig. 2 indicates that at the specified charge rate, it is lithium-ion depletion in the neighbourhood of the FeS electrode that limits the utilization of active materials. The concentration gradient from the electrode surface is directly proportional to the current density (and is given by Fick's first law). At low current densities, however, the concentration difference across the boundary layer may be so small that a freezing composition is not realized at the electrode. Hence there is a threshold current below which no electrolyte solidification will occur and the utilization should be 100%. From Fig. 2 this critical current is indicated to be 6 mA cm^{-2}. At higher currents a sufficient concentration difference for freezing to occur may be generated within the boundary layer, and the diffusion layer thickness (x) is seen to be inversely proportional to current density from

$$i = nFD\frac{(C_b - C_0)}{x} \qquad (2)$$

where C_b is the bulk concentration and C_0 is the surface concentration (= freezing composition at the end point). The utilization of active materials (U) is directly proportional to the amount of material removed from the electrolyte which (to a first approximation) is given by

$$\text{moles removed} = \tfrac{1}{2}(C_b - C_0)Ax \qquad (3)$$

for a volume element x cm thick adjacent to an electrode surface of A cm^2. Hence

$$U \propto x \qquad \text{and} \qquad i \propto \frac{1}{U}.$$

This type of behaviour is indicated in Fig. 2, but the maximum utilization realised was under 70%. This value was recorded at current densities of 8 mA cm^{-2} or under, and clearly a new process begins to limit the availability of lithium once the electrolyte constraints have been removed. Further experiments will be required to determine the nature of this process.

The effect of operating temperature on cell performance is shown in Fig. 4. Utilizations are increased from 13% to 30% to 50% at temperatures of 400, 450 and 500° C. Once more, the concept of limitations via solidification can be used successfully to interpret the data. Using the mole per cent change ratio required for freezing to occur at the FeS electrode (as measured from the phase diagram), the predicted utilizations corresponding to the above values would be 13%, 30% and 51%. The experimental data are in excellent agreement with these values.

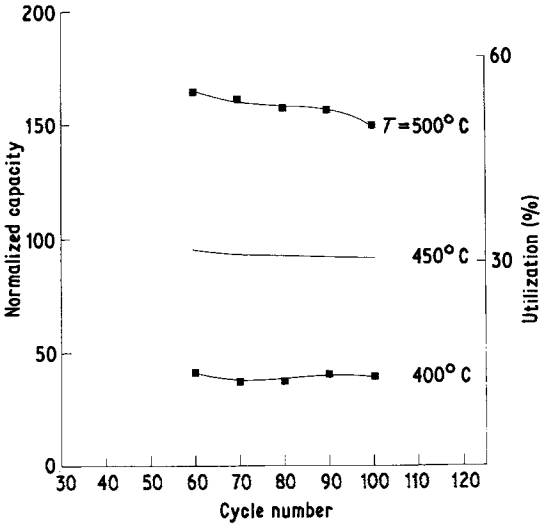

Fig. 4. Effect of operating temperature on cell capacity ($i_{charge} = i_{discharge} = 25$ mA cm^{-2}).

The avoidance of lithium excess and depletion problems may be achieved by employing all-lithium electrolytes (e.g. LiCl–LiF–LiI eutectics). This would encourage the better utilization of cell components and lead to an increase in the gravimetric energy density of cells.

Acknowledgement

The authors gratefully acknowledge the technical assistance provided by Mr A. C. Houston during this work.

References

[1] E. J. Cairns and H. Shimotake, *Science* **164** (1969) 1347.
[2] E. J. Cairns and J. S. Dunning, in *Proc. Symp. and Workshop on Advanced Battery Research and Design, Argonne National Laboratory*, March, ANL-76-8 (1976).
[3] W. J. Walsh *et al.*, in *Proc. 9th IECEC, ASME, New York* (1974).
[4] UK Patent 1510642, Improvements in or relating to high temperature secondary batteries (1978).
[5] Provisional UK Patent 12464/7, High temperature secondary cell.
[6] D. Birt, C. Feltham, G. Hazzard and L. Pearce, *Proc. 28th Power Sources Symposium, Atlantic City* (1978) p. 14.
[7] T. W. Olszanski and H. Shimotake, *Extended Abstracts of the 154th Meeting of the Electrochemical Society, Pittsburgh* (1978) p. 148.
[8] R. K. Quinn and N. R. Armstrong, *12th Int. Power Sources Symp., Brighton* (1980) paper 20.
[9] B. A. Askew, L. W. Eaton, F. Mariker and E. J. Chaney, *ibid* (1980) paper 22.
[10] J. Braunstein and C. E. Vallet, *J. Electrochem. Soc.* **126** (1979) 960.
[11] C. E. Vallet and J. Braunstein, *ibid* **125** (1978) 1193.
[12] C. E. Vallet, D. E. Heatherly and J. Braunstein, *ibid* **127** (1980) 1.